Development and evaluation of novel structurally simplified sialyl LewisX mimic-decorated liposomes for targeted drug delivery to E-selectin-expressing endothelial cells

(E−セレクチン発現内皮細胞への標的指向化薬物送達を目的とした新規構造単純化シアリルルイスＸミミック修飾リポソームの開発と評価)

- Digest Version -

2018

CHANTARASRIVONG CHANIKARN

Contents

Preface

E-selectin is a transmembrane glycoprotein that is expressed at extremely low levels in resting endothelial cells but its expression is strongly induced via transcriptional regulation by inflammatory cytokines, such as TNF-α and IL-1β [1-3]. Induced expression of E-selectin is involved in recruitment of leukocytes in inflamed tissues as well as formation of tumor microenvironment [4-6]. Therefore, augmented expression of E-selectin in endothelial cells is an attractive target for targeted delivery of specific drugs to inflamed endothelia including tumor vasculature [7-10].

E-selectin-directed drug delivery systems have mostly utilized sialyl LewisX (sLeX), a natural ligand of E-selectin. The sLeX-decorated liposomes and nanoparticles have successfully been demonstrated to be highly accessible delivery vehicles for E-selectin targeting both in vitro and in vivo [11-16]. However, their availability is hampered by the complexity and difficulty of sLeX synthesis [17-20]. To overcome these drawbacks, the design and development of structurally simplified analogs of sLeX (so-called sLeX mimics) is promising. Therefore, this study aimed to develop novel structurally simplified sLeX analog-decorated liposomes for targeted drug delivery to E-selectin-expressing endothelial cells, that could be a potential carrier to deliver drugs to inflamed or tumor endothelium.

In chapter 1, novel sLeX mimics were designed with structural simplification to overcome drawbacks of process-intensive chemical synthesis of native sLeX. The sLeX mimics were conjugated with phospholipids to be presented on the surface of liposomes and evaluated their targeting ability in inflammatory cytokine-treated endothelial cells. Among the sLeX mimic liposomes tested, the most potent sLeX mimic was studied further. In chapter 2, transport characteristics of the sLeX mimic liposomes were investigated in tumor spheroids with perfusable vascular network, which imitates solid tumor with blood circulation. In chapter 3, capability of the sLeX mimic liposomes in delivering drugs to E-selectin-expressing endothelial cells was investigated. In this context, anti-angiogenic drug loaded liposomes were prepared to investigate their characteristics and pharmacological effects. Details of the study will be discussed over the three chapters.

Chapter 1

Development and functional characterization of liposomes decorated with structurally simplified sLeX mimics

1-1. Introduction

E-selectin is a transmembrane glycoprotein that is expressed in endothelial cells. Its expression is extremely low in resting endothelial cells, but it is strongly induced by inflammatory cytokines such as TNFα and IL-1β [1-3]. The physiological function of E-selectin is to support leukocyte tethering and rolling on specific locations of the endothelium and allow for further strong integrin-mediated interactions. Leukocytes recruited at the site of inflamed tissues remove pathogens and cellular debris and produce growth factors for tissue repair. Therefore, the expression of E-selectin is involved as an initial trigger in attenuating acute inflammatory injury. However, it is also known that the same mechanism occurs during the development of tumor tissues [4-6]. Cancer cells and tumor stroma produce cytokines to activate the vascular endothelium, recruit and tame innate immune cells, and form a robust immunosuppressive network called the tumor microenvironment.

Augmented expression of E-selectin in endothelial cells at inflamed or tumor tissues is an attractive option for targeted delivery of specific drugs to these tissues. As has been reviewed elsewhere [7-10], several types of E-selectin-directed drug delivery systems, *i.e.*, lipid- or polymer-based nanoparticles decorated with anti-E-selectin antibodies and small molecular ligands, have been designed and functionally characterized. Studies on immunoliposomes bearing anti-E-selectin antibodies were conducted a relatively long time ago. The first demonstration of this concept was undertaken by Bendas et al. in 1998 [21], and was later expanded by their group and other groups [22-25]. However, sialyl Lewis^X (sLeX, Neu5Acα2-3Galβ1-4(Fucα1-3)GlcNAcβ) tetrasaccharide-decorated nanoparticles have also been studied [26-29]. sLeX is a naturally occurring E-selectin ligand and is found at the terminus of N- or O-glycans and glycolipids on the surface of leukocytes and tumor cells. Use of such a small molecular ligand is beneficial due to lower immunogenicity compared with the use of immunoliposomes [30,31]. However, although sLeX-decorated liposomes and nanoparticles have successfully been demonstrated to be highly accessible delivery vehicles for E-selectin targeting both in *vitro* and in *vivo* [11-15, 32], their availability is hampered by the complexity and difficulty of sLeX synthesis. The large-scale production of sLeX is costly, requires considerable technical expertise, and involves many synthesis steps [20, 33-35]. To overcome these drawbacks, the design and development of structurally simplified analogs of sLeX (so-called sLeX mimics) is promising.

Binding between sLeX and selectins have intensively been investigated in both functional and structural studies. Systematic replacement of the functional groups of sLeX with hydrogen revealed that all three OH groups of the Fuc, the 4- and 6-OH groups of the Gal, and the COO^- group of the NeuAc are required for sLeX to bind to E- and L-selectins [36,37]. In addition, it has been reported that the GlcNAc residue does not play a crucial role in binding. Crystallographic analysis of E-selectin and sLeX cocrystals supports the results of functional studies [38-40]. The 3- and 4-OH groups of the Fuc form a network of interactions with the selectin-bound Ca^{++} ion and several amino acid residues, while the 4- and 6-OH groups of the Gal and the COO^- group of the NeuAc are responsible for further hydrogen-bond formation. Accordingly, substitution of NeuAc with a negatively charged group, such as carboxymethyl, sulfate, and phosphate groups, on the 3' position of the Gal would be the most straightforward way to simplify the structure of sLeX [41-43]. Taking into account that the GlcNAc residue is not responsible for binding, Brandley, et al [44] previously proposed and demonstrated the feasibility of fucosylated 3'-sulfo-lactose as a potent and convenient sLeX mimic. Replacement of the Gal-GlcNAc disaccharide unit with lactose (*i.e.*, Gal-Glc) removes many initial steps.

In this chapter, based on reported structure-activity studies of sLeX and its mimics [36, 44-46], novel glycolipids that are available for E-selectin-targeted drug carriers were designed and synthesized in collaboration with Drs. Kiso and Ando, Gifu University. sLeX and its mimics were conjugated with 1,2-distearoyl-*sn*-glycero-3-phosphoethanolamine-polyethyleneglycol-2000 (DSPE-PEG), taking into account that the swollen layers formed with PEG chains are required for steric protection of particulate drug carriers [47-50]. Three fucosylated lactose derivatives modified on the 3' position of the lactose unit, *i.e.*, 3'-sulfo, 3'-carboxymethyl (3'-CM), and 3'-(1-carboxy)ethyl (3'-CE), were synthesized as sLeX mimics. On the basis of previous results of sLeX mimic development [44, 51], it has been expected that fucosylated 3'-sulfo-lactose would be a suitable targeting motif because of its binding affinity to E-selectin. The 3'-CM and 3'-CE analogs were newly designed as more chemically stable analogs than the 3'-sulfo (Scheme 1). These analogs retain the position of the COO^- group of NeuAc within sLeX and are expected to engage in hydrogen-bond formation similar to sLeX. In addition, the 3'-CE analog was anticipated to provide strong interaction to E-selectin because the methyl group of the 3'-CE group limits the free rotation of the COO^- group.

The sLeX mimics-DSPE-PEG conjugates were added to prepare liposome formulations intended for E-selectin-targeted drug delivery. Uptake characteristics of the sLeX mimic liposomes were delineated in a model of e-selectin overexpressing endothelial cells. A molecular mechanism underlying the binding of sLeX mimics with E-selectin were also confirmed in molecular dynamics studies.

1-2. Materials and Methods

1-2-a. Synthesis of sLeX mimic-linked phospholipids

The targeting motifs were synthesized using an efficient, stereoselective route (Scheme 1). First, 3-aminopropyl lactoside **1** was prepared according to a previously reported procedure [52], and it was then converted into the mono-hydroxy form **2** through a four-step reaction sequence. Next, compound **2** underwent α-selective fucosylation with donor **3** with the assistance of the synergistic solvent effect of CPME-CH_2Cl_2 [53], followed by replacement of the MBn group with an acetyl group and the acid hydrolysis of the isopropylidene group at C3' and C4', producing **4**. 3'-OH selective sulfonylation, carboxymethylation and 1-carboxyethylation via tin acetal formation and subsequent full deacylation produced 3'-sulfo and 3'-carboxymethyl and 3'-(1-carboxy)ethyl trisaccharides, respectively. Finally, they were conjugated with DSPE-PEG to create sLeX mimic targeting motifs **5**, **6** and **7**, respectively.

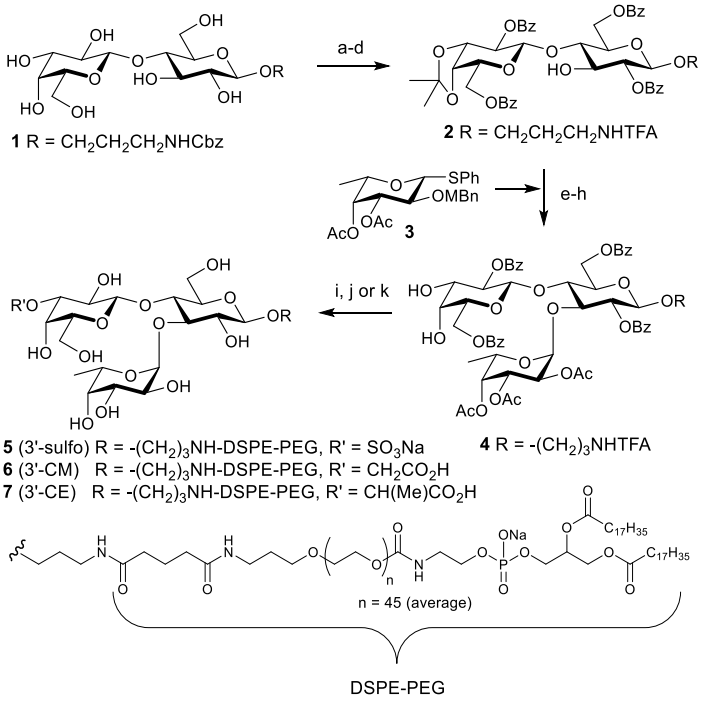

Scheme 1. Synthesis of sLeX mimic-linked phospholipids. (a) CSA/2,2-dimethoxypropane, acetone, MeCN, RT, 1 d, 63%; (b) H_2, 5% Pd/C/1,4-dioxane-H_2O (2:1), RT, 6 h; (c) TFAOMe, Et_3N/MeOH, RT, 4 h, 89% (2 steps); (d) BzCl/toluene-pyridine (4:3), 0°C, 1.5 h, 64%; (e) 3, NIS, TfOH, MS4Å/CPME-CH_2Cl_2 (1:1), -40°C, 1 d; (f) DDQ/CH_2Cl_2-H_2O (10:1), RT, 6 h; (g) Ac_2O/pyridine, RT, 2 h, 49% (3 steps); (h) 80% TFAOH aq./CH_2Cl_2, 0°C, 0.5 h, 98%; (i) i. *n*Bu_2SnO/toluene, reflux, 5 h; ii. SO_3·NMe_3/THF-DMF (4:1), RT, 15 h, 88% (2 steps); iii. 1 M NaOH aq./MeOH, RT, 21 h; iv. DSPE-PEG_{2000}-NHS /DMF-H_2O (4:1), RT, 1 h, 80% (2 steps); (j) i. *n*Bu_2SnO/toluene, reflux, 5 h; ii. ethyl bromoacetate, *n*Bu_4NI/toluene, 80°C, 5 h; iii. Ac_2O, DMAP/pyridine, RT, 6 h; iv. 1 M NaOH aq./MeOH, RT, 18 h; v. DSPE-PEG_{2000}-NHS /DMF-H_2O (4:1), RT, 1 h, 49% (5 steps); (k) i. *n*Bu_2SnO/toluene, reflux, 5 h; ii. BrCH(Me)CO_2Et, *n*Bu_4NBr/toluene, 100°C, 3 h; iii. Ac_2O, DMAP/pyridine, RT, 3 h, 44% (2 steps); iv. 1 M NaOH aq./MeOH, RT, 2 h; v. DSPE-PEG_{2000}-NHS, Me_3N/DMF-H_2O (3:1), RT, 1 h, 31% (2 steps). Cbz = benzyloxycarbonyl; TFA = trifluoroacetyl; Bz = benzoyl; MBn = *p*-methoxybenzyl; CSA = 10-comphorsulfonic acid; NIS = *N*-iodosuccinimide; CPME = cyclopentyl methyl ether; DDQ = 2,3-dichloro-5,6-dicyanobenzoquinone; DMF = *N,N*-dimethylformamide; DMAP = 4-dimethylaminopyridine; DSPE-PEG = 1,2-distearoyl-*sn*-glycero-3-phosphoethanolamine-polyethyleneglycol-2000; NHS = *N*-hydroxysuccinimidyl.

1-2-b. Preparation of liposomes

1,2-Distearoyl-sn-glycero-3-phosphocholine (DSPC) was purchased from Avanti Polar Lipids (Alabaster, AL). Cholesterol, methanol, and chloroform were purchased from Nacalai Tesque (Kyoto, Japan). DSPE-PEG-Fluorescein was prepared through the chemical reaction of DSPE-PEG-NH2 (NOF America Corporation, White Plains, NY) and Fluorescein-NHS (Thermo Fisher Scientific, Waltham, MA) following the protocol supplied by the manufacturer. DSPC (2.75 μmol/mL), cholesterol (1.95 μmol/mL), native sLeX- or sLeX mimic-linked DSPE-PEG (0.25 μmol/mL) and DSPE-PEG-Fluorescein (0.05 μmol/mL) were individually dissolved in chloroform-methanol (1:1). One milliliter of each solution was mixed in a 50-mL round-bottom flask. The solvent of the mixture was removed under reduced pressure using a rotary evaporator. The resultant lipid film was further vacuum-desiccated for at least 6 h. The lipid film was swollen using phosphate-buffered saline (PBS, Nissui Pharmaceutical, Tokyo, Japan) at room temperature for 30 min and suspended by shaking for 30 min in a water bath at 65°C. The suspension was sonicated in a bath-type sonicator (ASU-3M, AS ONE, Osaka, Japan) at 65°C for 10 min and then a tip-type sonicator (Ultrasonic generator US 300, Nissei, Tokyo, Japan) at an intensity of 200 W for 3 min. The suspension was then extruded 31 times through a 100-nm pore membrane equipped in an extruder (Avanti Mini-Extruder, Avanti Polar Lipids, Alabaster, AL) maintained at 65°C. The liposome solution was purified using a NAP-5 gel filtration column (GE Healthcare, Buckinghamshire, UK) equilibrated with PBS. After the

amount of phospholipids in the eluate was determined using a Phospholipids C-test Wako (Wako Pure Chemical Industry), the liposome concentration was adjusted to 500 nmol total lipid/mL. An aliquot of the stock solution was diluted 2.5 times with distilled water, and 750 μL of the solution was taken for measurement of the particle size and zeta potential of the liposomes in a Zetasizer Nano ZS (Malvern, Worcester, UK). Moreover, the fluorescence intensity of each liposome was determined at a total lipid concentration of 1 nmol/mL using a Fluoromax-4 spectrofluorometer (Horiba, Kyoto, Japan).

1-2-c. Cell culture

HUVECs were purchased from Kurabo Industry (Osaka, Japan) and cultured according to the protocol supplied by the manufacturer. HuMedia-EG2 (Kurabo, Osaka, Japan) was used as the culture medium. When the cells reached 70%–80% confluence, they were harvested using trypsin-EDTA, suspended in the culture medium, and plated on a dish. The rest of the cells was maintained in a flask for up to 3 generations. On day 1 after plating, the cells were pretreated with 100 ng/mL TNF-α (Life Technologies, Carlsbad, CA, USA) and 10 ng/mL IL-1β (Sigma-Aldrich, St. Louis, MO, USA) for 5 h, to induce E-selectin expression.

1-2-d. Evaluation of induction effect of TNF-α and IL-1β on E-selectin expression in HUVECs

HUVECs were harvested and suspended in the culture medium, and plated at 400,000 cells/mL in the 12-well plate on the day before experiments. TNF-α and IL-1β were added together or separately to the medium at a final concentration of 100 ng/mL and 10 ng/mL, respectively. After 5 h, cells were washed with 0.2 mL HEPES buffer (Kurabo, Osaka, Japan) and incubated with 0.2 mL of 0.0025% trypsin for 3-5 min at room temperature. The cells were then centrifuged, washed with 2 mL and resuspended with 0.3 mL of ice cold PBS. Thirty microliters of 10μg/mL anti-E-selectin antibody conjugated with FITC (Abcam, Cambridge, UK) was added and cells were incubated on ice for 30 min. The cells were washed 3 times with 2 mL and resuspended in 1 mL of ice cold PBS. Flow cytometry analysis was conducted using a FACSCanto II (BD Biosciences, San Jose, CA) with excitation and emission wavelength settings of 493 and 528 nm, respectively. Ten thousands gated cells were analyzed using fluorescence histogram with the BDFACSDiva software program.

1-2-e. Evaluation of the cellular uptake of liposomes

HUVEC were harvested, suspended in the culture medium, and plated at a density of 100,000 cells/0.5 mL in a 24-well plate on the day before experiments. Prior to uptake experiments, cytokines were added into the medium and the cells were incubated for another

5 h. At the onset of the uptake experiments, the culture medium was replaced with medium containing fluorescein-labelled liposomes (50 nmol total lipid/mL). Following incubation for the indicated time periods, the cells were washed with PBS and incubated with 0.3 mL of 0.0025% trypsin for 3–5 min at room temperature. The cells were then centrifuged and resuspended in 0.2 mL of ice-cold PBS. Flow cytometry analysis was conducted using a FACSCanto II with excitation and emission wavelength settings of 494 and 519 nm, respectively. Ten thousand gated cells were analyzed using a fluorescence histogram with the BDFACSDiva software program.

1-2-f. Confocal fluorescence microscopy analysis of the subcellular distribution of liposomes

HUVECs were harvested, suspended in the culture medium, and plated at a density of 40,000 cells/0.25 mL in an 8-well chamber slide on the day before the experiments. Prior to the experiments, cytokines were added into the medium and the cells were incubated for another 5 h. At the onset of the uptake experiments, the culture medium was replaced with medium containing fluorescein-labelled liposomes (50 nmol total lipid/mL). After incubating for 3 h, the cells were washed 3 times with PBS and fixed with 4% paraformaldehyde phosphate buffer solution (Nacalai Tesque, Kyoto, Japan). Fifteen minutes later, the cells were washed with PBS, mounted with Vectashield mounting medium containing DAPI (Vector laboratories Inc, Burlingame, CA), and observed using a confocal microscope (Nikon A1RMP/Ti-E/PFS, Nikon Instruments Inc., Melville, NY) equipped with NIS-elements AR 4.13.00 software. The excitation wavelength was set at 488.5 nm and 404 nm, and the emission wavelengths were scanned in the range of 500-550 nm and 425-475 nm for fluorescence and DAPI, respectively.

1-2-g. Evaluation of specific process of cellular uptake/association of liposomes in HUVECs

For cellular specific process of uptake study, HUVECs were harvested, and suspended in the culture medium, and plated at a density of 100,000 cells/0.5 mL in a 24-well plate on the day before the experiments. After 5h of cytokines treatment, the culture medium was replaced with that containing fluorescein-labeled liposomes (50 nmol total lipid/mL). After incubating for 3 h, the cells were prepared and analysed using flow cytometry with the same method as previous uptake study.

For specific process of cellular association study, HUVECs were harvested, suspended in the culture medium, and plated at a density of 40,000 cells/0.25 mL in a 48-well plate on the day before the experiments. Following a 5-h cytokine treatment, the culture medium was

replaced with an equal volume of Hank's buffered salt solution (HBSS) (Nissui Pharmaceutical, Tokyo, Japan) containing one of the anti-selectin antibodies (Abcam, Cambridge, UK) at a concentration of 10 μg/mL, and the cells were then incubated for 30 min on ice. Twenty-five microliters of 500 nmol total lipid/mL liposome solution was added at the onset of the cellular association study. Fifteen minutes later, the cells were washed twice with 0.3 mL of HBSS supplemented with 10% fetal bovine serum (FBS) and once with 0.3 mL of HBSS and then lysed with 0.1 mL of an aqueous lysis buffer composed of 0.05% Triton X-100, 0.075% EDTA, and 1.21% Tris for 15 min on a shaker. The lysates were transferred to a 96-well plate, and their fluorescence intensity was determined using an ARVO MX microplate fluorometer (Perkin Elmer, Waltham, MA) with excitation-emission wavelengths set at 485 and 535 nm, respectively. The protein concentration in 20-μL aliquots of the lysate was measured using the Protein Quantification Kit-Wide Range (Dojindo Molecular Technologies, Rockville, MD). In addition, the inhibitory effects of anti-selectin antibodies were statistically evaluated using a one-way analysis of variance with Dunnett's post hoc test.

1-2-h. Molecular dynamics simulation

The structure of the sLeX-E-selectin cocrystal (PDB: 4CSY) [40] was used as a template to investigate the molecular binding of sLeX mimics with E-selectin. A molecular dynamics (MD) calculation of the solvated protein-ligand complex was performed using the GROMACS 5.0.4 package [54]. The AMBER-ff99SB force field [55] and the AMBER-GAFF [56]/AM1-BCC [57] were assigned for E-selectin and ligand molecules, respectively. Each complex structure was neutralized and placed in a TIP3P [58] water box, with a margin of 10 Å between the protein and the boundaries of the periodic box. The particle mesh Ewald method with a cut-off of 8 Å was used to calculate long-range electrostatic interactions. MD simulations of 100 ps for the system relaxation under constant NVT conditions at 300 K and 400 ps for water molecule density equilibration under constant NPT conditions at 1 bar and 300 K were performed before data collection. Subsequently, an MD simulation of 2 ns was performed under constant NVT conditions at 300 K, and the complex structures were extracted in the 201 snapshots taken every 10 ps. This MD simulation scheme was replicated three times, and the analyses for hydrogen-bond formations and distributions of dihedral angles were performed in a total of 603 snapshots.

1-3. Results and Discussion

1-3-a. Synthesis of sLeX mimic-linked phospholipids

Novel glycolipids bearing sLeX mimics were designed and synthesized (Scheme1). The common intermediate 4 was synthesized in 18 steps from the starting materials (Lac and Fuc) and target compounds 5, 6, 7 were synthesized in 3 or 4 steps from 4 (total 21 or 22 steps). This synthetic route is shorter than that of the glycolipid conjugated with native sLeX tetrasaccharide (31 steps from GlcNH2, Gal, Fuc, and NeuAc) [59]. In addition, the number of glycosidation reactions, which require high expertise and laborious purification of the reaction product, were reduced to 2 times in the synthetic route, compared to that of sLeX tetrasaccharide (4 times). Therefore, the large-scale synthesis of the mimics would be possible by the synthetic route.

1-3-b. Physicochemical characteristics of native and mimic sLeX liposomes

Table 1 summarizes the particle size and zeta potential of the prepared liposomes. The average diameter was similar in all the liposomes, ranging from 96.4 to 106.4 nm. Their polydispersity indices were no more than 0.19, indicating that liposomes with a uniform size distribution were obtained by employing an extrusion method following the hydration-sonication method. Whereas the PEG liposome was nearly neutral with a zeta potential of −6.92 ± 1.23 mV, all liposomes bearing the native or mimic sLeX residues were highly negative with regard to surface charge, but the negative charges associated with native or mimic sLeX were not significantly different. The fluorescence intensities of all prepared liposomes were comparable but, to be more precise, were employed for normalization of cellular uptake.

Table 1. Physicochemical characteristics of native and mimic sLeX liposomes

Liposome[a)]	Average diameter (nm)	PDI[b)]	Zeta potential (mV)
PEG	102.53 ± 0.46	0.16	–6.92 ± 1.23
Native sLeX-PEG	98.45 ± 1.01	0.16	–24.5 ± 1.1
3'-sulfo sLeX mimic-PEG	106.37 ± 1.46	0.19	–23.97 ± 0.85
3'-CM sLeX mimic-PEG	96.35 ± 0.51	0.17	–23.03 ± 1.7
3'-CE sLeX mimic-PEG	102.33 ± 0.71	0.11	–24.70 ± 1.1

Results of diameter and zeta potential are expressed as mean ± standard deviation (SD) of three samples.

a) *PEG, polyethylene glycol; 3'-CM, 3'-carboxymethyl; 3'-CE, 3'-(1-carboxy)ethyl.*

b) PDI, polydispersity index.

1-3-c. Induction effect of TNF-α and IL-1β on E-selectin expression in HUVECs

Cytokine-stimulated HUVECs have often been used as a model of E-selectin-expressing inflammatory endothelium [60-64]. This study was done to confirm effect of cytokines on E-selectin expression of HUVECs. **Figure 1** shows that treatment of HUVECs with TNF-α or IL-1β increased the expression of E-selectin on their surface by 6.6 and 7.5 times, respectively, whereas combined treatment of both of the cytokines resulted in additive induction of expression of the E-selectin 16.9 times. This result indicated that dual pretreatment with TNFα and IL-1β provided greater E-selectin induction than pretreatment with single cytokines. Indeed, the binding of a fluorescein-labeled anti-E-selectin antibody to HUVECs treated with dual cytokines was more than twice that of HUVECs treated with either TNF-α or IL-1β alone. Therefore, HUVECs pretreated with both TNF-α and IL-1β are best suited for this experiment.

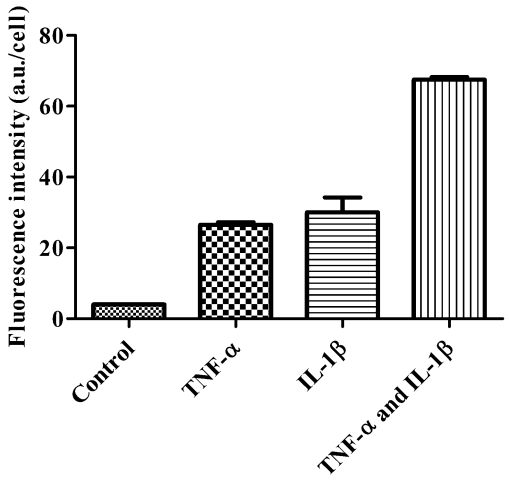

Figure 1. Effect of TNF-α and IL-1β on the expression of E-selectin on the surfaces on HUVECs. Results are expressed as mean + SD of three samples.

1-3-d. Uptake in cytokine-treated HUVECs

Figure 2A shows the time course of the uptake of native and mimic sLeX liposomes in proinflammatory cytokine-treated HUVECs. The cellular uptake of all tested liposomes increased linearly over 4 h. The uptake rate calculated from the slope was highest with the 3'-CE sLeX mimic liposomes (105.2-fold higher than that of the PEG liposome), followed by the 3'-sulfo sLeX mimic (90.1-fold), native sLeX (85.1-fold), and 3'-CM sLeX mimic liposomes (25.5-fold). Hereafter, the cellular uptake of the liposomes was evaluated at 3 h.

Figure 2B shows the concentration dependence of the liposome uptake. The uptake of native and mimic sLeX liposomes obeyed nonlinear kinetics within the concentration range tested (0.025–0.2 μmol total lipid/mL). The Eadie–Hofstee plot analysis indicated that the Michaelis–Menten constants (Km) were 0.011, 0.020, 0.025, and 0.057 μmol total lipid/mL for the 3'-CE sLeX mimic, native sLeX, 3'-sulfo sLeX mimic, and 3'-CM sLeX mimic liposomes,

respectively (**Figure 3**). The order of the affinity-related constant values corresponded to that of the uptake rate. The Km values for each type of liposome presumed that all of the ligand residues, i.e., 5 mol%, were available for specific binding. The resulting Km values are not strictly accurate because this approach does not consider what percentage of these residues are directed to the liposome surface, but it allows for a relative comparison in affinity among the liposomes. Ohmoto et al. [45] and Wada et al. [65] have investigated the binding of the 3'-sulfo sLeX mimic and native sLeX to selectin-IgG chimeras in enzyme-linked immunosorbent assay (ELISA) inhibition assays. The half maximal inhibitory concentration (IC50) values for the reported analogs [45, 65] were in the same concentration range as the Km values obtained in the current study. However, these previous studies [45, 65] have indicated that the 3'-sulfo sLeX mimic has slightly less potency than the native sLeX in binding to E-selectin, whereas our present results indicate that both are almost comparable in terms of Km. This inconsistency may be due to differences in experimental conditions: we used liposome-conjugated sLeX mimics instead of free sLeX mimics and a cell-based but not a cell-free assay.

Results from above indicating that the highest uptake was exhibited by the 3'-CE sLeX mimic liposome, whereas the 3'-CM sLeX mimic liposome had the lowest activity. Interestingly, the substitution of a proton in the carboxymethylene with a methyl group led to totally different outcomes in terms of the uptake of these 2 carboxyl-type sLeX mimic-decorated liposomes, in other words, substitution of methyl group in the carboxymethylene greatly improved the cellular uptake in E-selectin-overexpressing HUVECs.

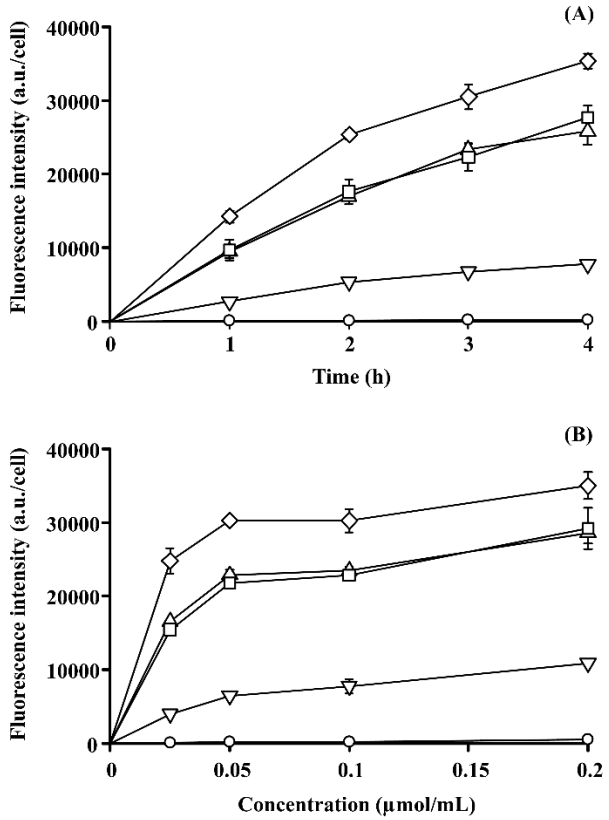

Figure 2. Time-course analyses (A) and concentration dependence (B) of the uptake of fluorescein-labeled liposomes in HUVECs treated with TNF-α and IL-1β for 5 h. Symbols: ○, PEG liposome; △, native sLeX liposome; □, 3'-sulfo sLeX mimic liposome; ▽, 3'-CM sLeX mimic liposome; ◇, 3'-CE sLeX mimic liposome. Results are expressed as mean ± SD of three samples.

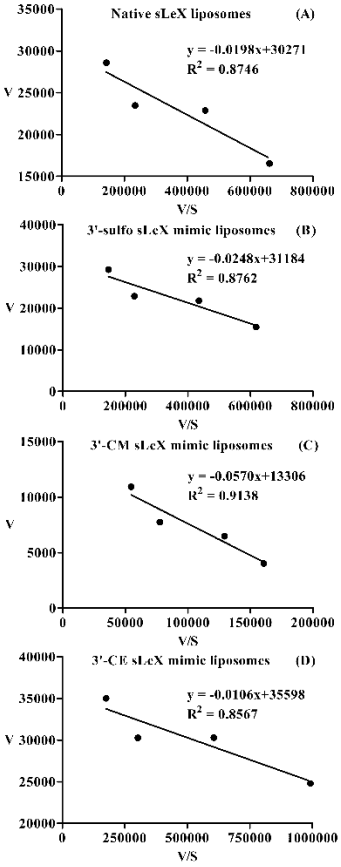

Figure 3. Eadie–Hofstee diagrams of the uptake of (A) native sLeX, (B) 3'-sulfo sLeX mimic, (C) 3'-CM sLeX mimic, and (D) 3'-CE sLeX mimic liposomes in HUVECs pretreated with 100 ng/mL TNF-α and 10 ng/mL IL-1β for 5 h. The ordinate and abscissa represent the uptake rate (v) and the uptake rate divided by liposome concentration (v/s), respectively. The regressed equation, together with its regression coefficient, is shown in each panel, where

$$v = -K_m \cdot \frac{v}{s} + V_{max}$$

To confirm the cellular internalization of the liposomes, confocal fluorescence microscopy was employed. **Figure 4** shows the subcellular distribution of fluorescence signals in proinflammatory cytokine-treated HUVECs at 3 h following the application of each type of liposome. In contrast to PEG liposomes, high fluorescence signals were detected throughout the entire cell interior when native sLeX or 3'-CE sLeX mimic liposomes were applied. In

addition, bright granular spots of fluorescence were found in the subcellular compartment, suggesting endocytic internalization of sLeX liposomes. Although fluorescent intensity of 3'-CE sLeX mimic liposomes was significantly greater than that of native sLeX liposomes, profiles of subcellular fluorescence distribution were similar. Thus, structural simplification of the ligand was unlikely to functionally alter the cellular internalization process of sLeX liposomes.

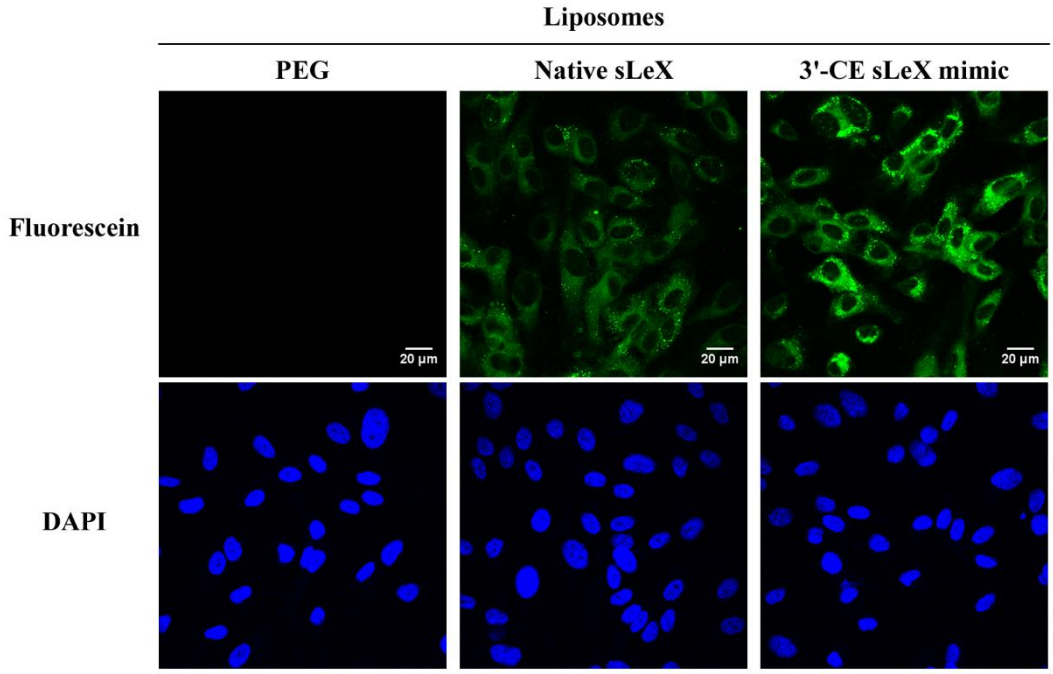

Figure 4. Confocal fluorescence microscopy of subcellular distribution of PEG, native sLeX, and 3'-CE sLeX mimic liposomes in HUVECs treated with TNF-α and IL-1β. The images were taken at 3 h following application of the liposomes to the cells. The liposomes were labeled with DSPE-PEG-Fluorescein (green color). The cells were stained with DAPI (blue) following fixation with 4% paraformaldehyde. The bar represents 20 μm.

1-3-e. Specific process of cellular uptake/association of liposomes in HUVECs

Figure 5 shows that cellular uptake of native and mimic sLeX liposomes in cytokine-treated HUVECs was 2 orders of magnitude higher than that in nontreated HUVECs, whereas the uptake of PEG liposomes was similar in both cytokine-treated and nontreated cells. Such a big difference is possibly due to augmented expression of E-selectin by treatment with TNF-α and IL-1β. The cellular uptake of 3'-CE sLeX mimic liposomes was also compared in between different ligand densities. The uptake of 3'-CE sLeX-mimic liposome was only 1.2 times different in between the two concentrations of 2.5% and 5%, suggesting that the ligand density of 5% would be high enough.

To confirm whether the increased uptake is due to E-selectin mediated processes, the effect of specific antibodies on the cellular association of the liposomes was investigated. **Figure 6** shows the cellular association of native and mimic sLeX liposomes in the presence and absence of specific antibodies against E-selectin, P-selectin, or L-selectin (10 μg/mL). The anti-E-selectin antibody inhibited the cellular association of native sLeX, 3'-sulfo sLeX mimic, and 3'-CE sLeX mimic liposomes by 70%, 72.7%, and 91.7%, respectively, whereas significant inhibition did not occur for the 3'-CM sLeX mimic liposome. In contrast, neither the anti-P-selectin nor anti-L-selectin antibodies affected the cellular association of any of the liposomes. Therefore, the uptake of native and mimic sLeX liposomes was considered to be mediated mostly by E-selectin, the expression of which was upregulated by pretreatment with TNF-α and IL-1β. An anti-P-selectin antibody did not affect the association of any of the liposomes tested, despite previous reports that sLeX is a P-selectin ligand [66-68]. This is likely because of the low expression of P-selectin in HUVECs regardless of treatment with inflammatory cytokines such TNF-α and IL-1β [69, 70].

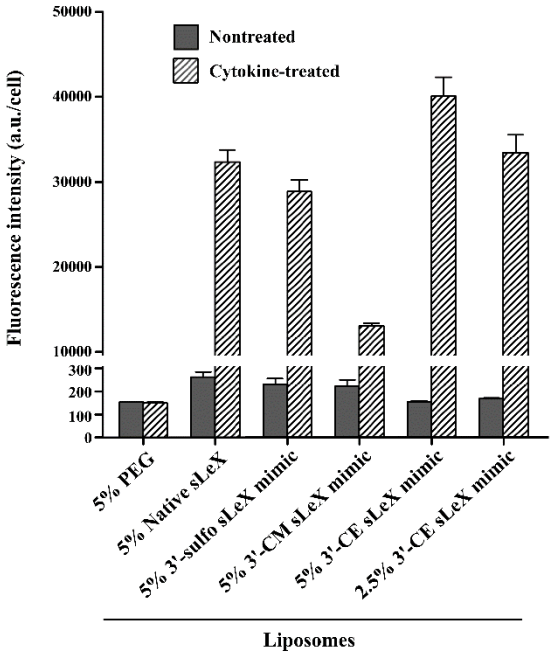

Figure 5. Uptake of fluorescein-labeled liposomes for 3 h in HUVECs treated or nontreated with TNF-α and IL-1β. Results are expressed as mean + SD of three samples.

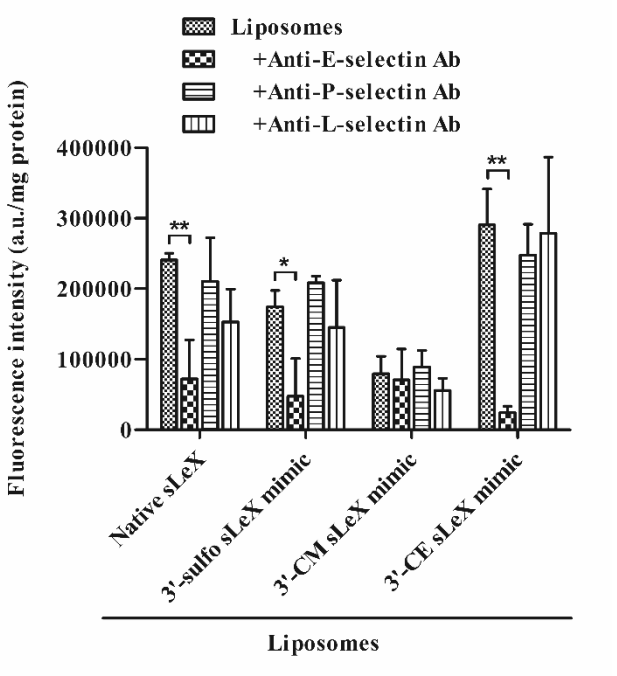

Figure 6. Inhibition by anti-selectin antibodies of the association of fluorescein-labeled native and mimic sLeX liposomes with HUVECs treated with TNF-α and IL-1β. Results are expressed as mean + SD of three samples. *P<0.05. **P<0.01.

1-3-f. Molecular dynamics simulation of the interaction of native and mimic sLeX with E-selectin

Two new sLeX mimics (i.e., 3'-CM and 3'-CE sLeX mimics) were designed and synthesized in this study, which have been modified from previously reported carboxyl-type mimics [71, 72] by taking into consideration the ease and efficiency of their synthesis. Interestingly, the substitution of a proton in the carboxymethylene with a methyl group led to totally different outcomes in terms of the uptake of carboxyl-type sLeX mimic-decorated liposomes in E-selectin-overexpressing HUVECs (**Figure 1**). To gain insight into the mechanism, MD simulation studies were conducted.

Differences in binding free energy between the liposomes estimated from experimental Km values were at most ~1 kcal/mol, which is considered to be too small for quantitative evaluation by MD simulation. Therefore, qualitative evaluations on binding modes to E-selectin, i.e., hydrogen-bond formation and distribution of dihedral angles were conducted. Even though, many interactions occur in the binding of sLeX to E-selectin, including calcium-mediated binding of the 2- and 3-hydroxyl groups of fucose, hydrogen bonding of hydroxyl groups of fucose and galactose to Glu80 or Tyr94, and hydrogen bonding between the carboxyl group of NeuAc and Arg97 [37, 73], it was sufficient to pay attention to interactions between the 3'-position group of galactose and the amino acid residues of E-selectin as a result of the structures of native sLeX and the 3'-CM and 3'-CE sLeX mimics.

One identified mode of interaction was the formation of hydrogen bonds between the 3'-position group of the sLeX mimics and amino acid residues of E-selectin, for which the phenolic oxygen of Tyr48 (Tyr48-Oη) and the guanidine nitrogens of Arg97 (Arg97-Nε, Arg97-Nη) were responsible (**Figure 7**). Taking the cut-off for hydrogen-bond distance as 3.2 Å, the probability of each intermolecular hydrogen-bond formation was calculated from a total of 603 snapshots during MD simulations (**Table 2**). The 3'-CM sLeX mimic can form a hydrogen bond only with Tyr48-Oη, with much lower probability compared with the native sLeX and 3'-CE sLeX mimic. In contrast, the 3'-CE sLeX mimic can form hydrogen bonds simultaneously with all three possible atoms. This is in agreement with the higher uptake of the 3'-CE sLeX mimic liposome in cytokine-stimulated HUVECs compared with the other liposomes.

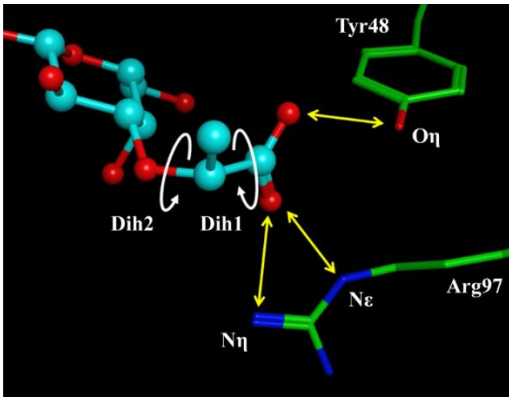

Figure 7. A snapshot of the molecular interaction of the 3'-position group of the 3'-CE sLeX mimic with the amino acid residues of E-selectin.

Table 2. Probability of each intermolecular hydrogen-bond formation between the 3'-position group of sLeX mimics and the amino acid residues of E-selectin

	Hydrogen-bond formation probability (%)		
	Tyr48-Oη	Arg97-Nε	Arg97-Nη
Native sLeX	93.7	61.9	29.4
3'-sulfo sLeX mimic	52.7	49.8	10.8
3'-CM sLeX mimic	57.5	20.4	11.3
3'-CE sLeX mimic	84.9	77.6	81.8

In addition, the probability density distribution for two dihedral angles, i.e., the dihedral angles of O(carboxylate)-C-C-O(ether) (Dih1) and of C(carboxylate)-C-O(ether)-C(galactose) (Dih2), was calculated to evaluate the rotational degrees of freedom of the 3'-position functional groups. The Dih1 for native sLeX provided a single-peak distribution around –70°, indicating highly restricted rotation of the carboxylate group. The 3'-CE sLeX mimic mostly kept the carboxylate plane at the same angle as that of native sLeX, although the carboxylate plane could sometimes be inverted (indicated by a small peak at 80°). However, the distribution of the Dih1 for the 3'-CM sLeX mimic was much broader, implying that its carboxylate group is more freely rotatable. With regard to the Dih2, no remarkable peaks were observed with any of the ligands (**Figure 8**). When the 3'-CE sLeX mimic has the primary conformation, the terminally branched methyl group is oriented and faces the bulk hydrophilic solution in spite of its hydrophobic nature (**Figure 9**). Since this state is entropically unfavorable, the 3'-CE sLeX mimic molecule might be pushed toward the binding pocket of E-selectin by a hydrophobic effect. In contrast, the carboxyl group of native sLeX had a fixed direction because of the bulky sugar group. Although the conformation is stable in native sLeX, such an entropic effect as that seen in the 3'-CE sLeX mimic would not exist because its

sugar group is hydrophilic. Therefore, differences in the interaction of the ligands with bulk water might explain the stronger binding of the 3'-CE sLeX mimic to E-selectin.

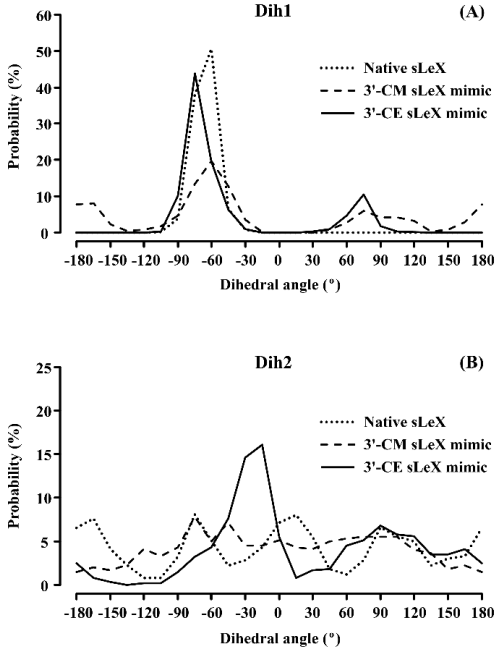

Figure 8. Density distribution for the dihedral angles of O(carboxylate)-C-C-O(ether), Dih1 (A) and of C(carboxylate)-C-O(ether)-C(galactose), Dih2 (B) in the 3'-position functional group of native sLeX (dotted line), 3'-CM sLeX mimic (dashed line), and 3'-CE sLeX mimic (solid line) complexed with E-selectin. The distribution profiles were obtained from a total of 603 snapshots (every 10 ps for 2 ns, 3 runs) during MD simulation.

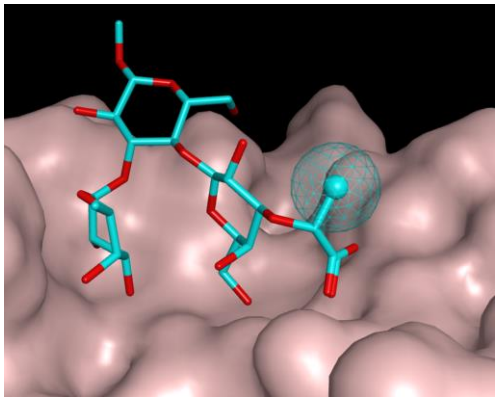

Figure 9. Binding position of the 3'-CE sLeX mimic. The terminally branched methyl group is shown in a mesh sphere.

1-4. Conclusion

Novel sLeX mimics were successfully developed with a less complicated synthesis and improved activity. In a liposome delivery system, the 3'-CE sLeX mimic liposome showed the highest uptake in E-selectin-overexpressing HUVECs. MD simulation studies demonstrated that the 3'-CE sLeX mimic is more strongly bound to E-selectin than native sLeX, because of the higher probability of hydrogen-bond formation. Therefore, the 3'-CE sLeX mimic liposome has a greater potential for targeted drug delivery to the endothelium of inflamed tissues and tumor tissues.

Chapter 2

Transport characteristics of 3’-(1-carboxy)ethyl sialyl LewisX mimic liposomes in tumor spheroids with a perfusable vascular network

2-1. Summary

Tumor vasculature targeting is one of the promising approaches in cancer therapy. The therapeutic concept that tumor growth can be suppressed by shutting out the supply of oxygen and nutrients can apply to any solid tumors. With regard to tumor vessel-targeted delivery systems, it is beneficial that the carriers can interact with the target cells without necessity of penetrating an endothelial barrier [74-76]. However, information on mechanistic aspects of local disposition behaviors in tumor tissues is still limited even though several tumor vasculature models including dorsal chamber models and tissue-isolated perfused tumor have been developed. It is because preparation of in vivo models is time consuming and prone to variability [77-82].

In this chapter, tumor spheroids with a perfusable vascular network were prepared in microfluidic device for evaluating the local disposition behavior of liposomes in solid tumors. Dynamic disposition behavior of 3'-CE sLeX mimic liposomes, the most potent in E-selectin–mediated delivery in chapter 1, was evaluated in this model. A co-culture spheroid comprising of HUVECs, lung fibroblast, and MCF-7 breast cancer cell line, was prepared and loaded into a microfluidic device. With culture time, angiogenic sprouts were branched and elongated from the spheroid and two-sided open microchannels to attract each other. On day 7, a perfusable continuous vascular network was completely developed in the microfluidic device. Quantitative reverse transcriptase polymerase chain reaction (qRT-PCR) demonstrated that E-selectin expression was similar in both MCF-7-present and MCF-7-absent spheroids, indicating that MCF-7 itself cannot stimulate E-selectin expression of HUVECs in spheroid. However, treatment with supplemented inflammatory cytokines greatly induced the E-selectin expression of the spheroids. Real-time imaging of fluorescent-labeled liposomes were done to investigate their dynamic disposition behavior in the vascularly perfused spheroid. 3'-CE sLeX mimic liposomes and PEG-liposomes exhibited almost the same behavior in tumor spheroid without cytokine treatment. However, when the spheroid was pretreated with inflammatory cytokines, significant amount of 3'-CE sLeX mimic liposomes distributed along endothelial cells and their vicinity but not with PEG-liposomes. Considering that inflammatory cytokines induce E-selectin expression regardless of 2D or 3D culture, the augmented uptake of 3'-CE sLeX mimic liposomes would be E-selectin-mediated. It would be

interesting to visualize the interaction of 3’-CE sLeX mimic liposomes with endothelium under dynamic flow condition.

In conclusion of this chaper, a novel tumor vasculature model for evaluating the function of drug delivery systems was developed on microfluidic device. Only under the cytokine-treated condition, 3’-CE sLeX mimic liposomes, which can be strongly associated with E-selectin-expressing cells, were taken up much more greatly than PEG liposomes. Assuming that in vivo tumor endothelium exclusively expresses E-selectin, 3’-CE sLeX mimic liposomes would be a promising carrier for targeted drug delivery to tumor endothelium.

Chapter 3

Anti-angiogenic drug delivery to E-selectin expressing endothelial cells by using 3’-(1-carboxy)ethyl sialyl LewisX mimic liposomes

3-1. Summary

Anti-angiogenic therapy is one of the most effective approaches for the treatment of various types of cancers [83-85]. However, it may induce adaptive tumor microenvironmental defense mechanisms, leading to drug resistance or invasion. While combinatorial therapies using different drug targets are suggested to overcome the resistance [86, 87], attention has also been paid to targeted drug delivery to improve the efficacy of drugs in anti-angiogenic therapy [88-91].

Everolimus (EVE), a mammalian target of rapamycin (mTOR) inhibitor, is a drug with anti-angiogenic property that was used in this study. EVE was encapsulated in PEG liposomes and 3'-CE sLeX mimic liposomes, a promising carrier for drug delivery to tumor endothelial cells indicated from results of chapter 2. In this chaper, their physicochemical properties, cellular uptake, and pharmacological effects were investigated in HUVECs stimulated with inflammatory cytokines. Cellular uptake of EVE/3'-CE sLeX mimic liposomes increased steadily and almost caught up with the uptake of plain EVE at 3 h, which was higher than the uptake in control pegylated liposomes. Anti-E-selectin antibody inhibited only the uptake of EVE/3'-CE sLeX mimic liposomes and the uptake amount under antibody blockage was similar to EVE/PEG liposomes, implying that improved uptake of EVE/3'-CE sLeX mimic liposomes would be primarily due to an E-selectin-mediated uptake process. However, the difference between the uptake of the two liposome formulations was not so large as that seen with fluorescein-labeled liposomes in chapter 1, leakage of EVE from liposomes could not be ruled out. Cell migration and capillary tube formation of HUVECs, referring to their angiogenic activity, were suppressed significantly by the EVE/3'-CE sLeX mimic liposomes compared to the control. In addition, Thr389 phosphorylation of pS6 kinase, as a marker of mTOR activity, was remarkably suppressed to less than endogenous levels by the EVE/3'-CE sLeX mimic liposomes. However, EVE/PEG liposomes had partial suppression effects.

These results show that the EVE/3'-CE sLeX mimic liposomes were intracellularly taken up by E-selectin and prompted anti-angiogenic effects of EVE involved in the mTOR signaling pathway. However, moderate retention of EVE in the liposomes might limit the targeting ability of 3'-CE sLeX mimic liposomes.

Summary

The aim of this study was to develop E-selectin-targeted liposomes, by design of novel structurally simplified sLeX mimics as ligands, for delivering drugs to inflamed endothelium including tumor vasculature. The findings of each chapter are summarized as follows

Chapter 1: Development and functional characterization of liposomes decorated with structurally simplified sLeX mimics

Structurally simplified novel sLeX analogs were designed and linked with DSPE-PEG for E-selectin-mediated liposomal delivery. The sLeX structural simplification strategies include (1) replacement of the Gal-GlcNAc disaccharide unit with lactose to reduce many initial steps and (2) substitution of neuraminic acid with a negatively charged group, i.e., 3'-sulfo, 3'-carboxymethyl (3'-CM), or 3'-(1-carboxy)ethyl (3'-CE). While all the liposomes developed were similar in particle size and charge, the 3'-CE sLeX mimic liposome showed the highest uptake mediated primarily by E-selectin in inflammatory cytokine-treated HUVECs, being even more potent than native sLeX-decorated liposomes. MD simulation studies demonstrated that the 3'-CE sLeX mimic is more strongly bound to E-selectin than native sLeX, because of the higher probability of hydrogen-bond formation. Therefore, the 3'-CE sLeX mimic liposome has a greater potential for targeted drug delivery to the endothelium of inflamed tissues.

Chapter 2: Transport characteristics of 3’-(1-carboxy)ethyl sialyl LewisX mimic liposomes in tumor spheroids with a perfusable vascular network

Tumor spheroids with a perfusable vascular network were prepared in microfluidic device as tumor vasculature model that allows to analyze the local disposition behavior of liposomes in solid tumors. The endothelial cells in the spheroid formed a continuous vascular network with angiogenic sprouts branchedly elongated from open microchannels of the device. Treatment with TNFα and IL-1β could increase E-selectin expression in tumor spheroid. Perfusion study of fluorescent-labeled liposomes shows that 3’-CE sLeX mimic liposomes significantly distributed along endothelial cells and their vicinity in the spheroid under flow condition. In contrast, control pegylated liposomes showed low retention due to weak binding. These results suggested that 3’-CE sLeX mimic liposomes were taken up in perfused tumor spheroid much higher than PEG liposomes. Therefore, the 3’-CE sLeX mimic liposomes has a potential for targeted drug delivery to tumor endothelium.

Chapter 3: Anti-angiogenic drug delivery to E-selectin expressing endothelial cells by using 3'-(1-carboxy)ethyl sialyl LewisX mimic liposomes

Everolimus-encapsulated 3'-CE sLeX mimic liposomes (EVE/3'-CE sLeX mimic liposomes) was developed and evaluated in inflammatory cytokines-treated HUVECs. The uptake of EVE in 3'-CE sLeX mimic liposomes increased steadily and almost caught up with the uptake of plain EVE at 3 h, which was higher than that in PEG liposomes. The improved uptake was confirmed as E-selectin-mediated endocytotic processes. However, the difference between the uptake of the two liposome formulations was not so large, leakage of EVE from liposomes could not be ruled out. Cell migration and capillary tube formation of HUVECs, referring to their angiogenic activity, were suppressed significantly by the EVE/3'-CE sLeX mimic liposomes compared to the control. Thr389 phosphorylation of pS6 kinase, as a marker of mTOR activity, was remarkably suppressed to less than endogenous levels by EVE/3'-CE sLeX mimic liposomes. These studies demonstrated that EVE/3'-CE sLeX mimic liposomes were intracellularly taken up by E-selectin and prompted anti-angiogenic effects of EVE involved in the mTOR signaling pathway. However, moderate retention of EVE in the liposomes might limit the targeting ability of 3'-CE sLeX mimic liposomes.

In conclusion, the novel structurally simplified sLeX mimic-decorated liposomes were successfully developed as a potential carrier to deliver drugs targeting to inflamed endothelium including tumor vasculature.

Acknowledgement

My five years in Japan have been the most challenging years of my life. Obtaining my Master's degree and Doctoral Degree would not have been possible without the guidance, support, and help of wonderful people that I have met throughout this journey. I would like to express my sincerest gratitude to the following:

To Professor Emeritus Mitsuru Hashida (Institute for Advanced Study, Kyoto University) for accepting me to this laboratory and giving me many opportunities in my student life.

To Professor Fumiyoshi Yamashita (Graduate School of Pharmaceutical Sciences, Kyoto University) for his supervision, great ideas in research, and constructive discussion. I learned a lot of doctoral skills from him that will surely help me in my future career.

To Senior Assistant Professor Yuriko Higuchi (Graduate School of Pharmaceutical Sciences, Kyoto University) for her guidance, advice, continuous support, and valuable discussion. I have learned many experiment skills from her that will certainly help me work smoothly in my researcher life.

To Professor Hiromune Ando (Center for Highly Advanced Integration of Nano and Life Sciences (G-CHAIN), Gifu University) and Associate Professor Akiharu Ueki (Faculty of Pharmaceutical Sciences, Aomori University) for their support in synthesis. This thesis would not be complete without their help.

To Professor Isao Nakanishi (Faculty of Pharmacy, Kindai University) and Assistant Professor Shinya Nakamura (Faculty of Pharmacy, Kindai University) for providing Molecular dynamic simulation, which really helped improve this thesis.

To Associate Professor Ryuji Yokokawa (Faculty of Engineering, Kyoto University) and Dr. Ryu Okada (Faculty of Engineering, Kyoto University) for their support in spheroid development, which is very important for this thesis, their hospitality, and their encouraging words.

To the Japanese Government and MEXT for the financial support. I hope they would continue providing opportunities to others like me who want to pursue their graduate studies in Japan.

To my lab mates for their assistance in my experiments and my Japanese friends for helping me with matters in Japanese that I do not understand.

To my Thai friends for making my life in a foreign country less difficult and enjoyable.

To those who wish me all good things that I cannot mention all here, thank you.

To my family - my mom Sarin, my brother Issara, and my family in the Philippines and Australia - for their unconditional love, prayers, encouraging, and wishes. They gave me strength to overcome all obstacles. My success and achievements are for you.

To my husband, Jason, for being by my side in every situation, supporting me the best in both physical and mental health, making my life better and happier, helping, caring, and loving me unconditionally.

Finally, to Gods for blessing me and being my spiritual anchor.

List of Publications

Synthesis and functional characterization of novel sialyl LewisX mimic-decorated liposomes for E-selectin-mediated targeting to inflamed endothelial cells.

Chanikarn Chantarasrivong, Akiharu Ueki, Ryutaro Ohyama, Johan Unga, Shinya Nakamura, Isao Nakanishi, Yuriko Higuchi, Shigeru Kawakami, Hiromune Ando, Akihiro Imamura, Hideharu Ishida, Fumiyoshi Yamashita, Makoto Kiso, Mitsuru Hashida.

Molecular Pharmaceutics. 2017. 14, 1528-1537.

Disposition behaviors of sialyl LewisX mimic-decorated liposomes in tumor spheroids with a perfusable vascular network.

Chanikarn Chantarasrivong, Ryu Okada, Yuriko Higuchi, Miku Konishi, Naoko Komura, Hiromune Ando, Ryuji Yokokawa, Fumiyoshi Yamashita.

Manuscript in preparation

Sialyl LewisX mimic-decorated liposomes for anti-angiogenic everolimus delivery to E-selectin expressing endothelial cells.

Chanikarn Chantarasrivong, Yuriko Higuchi, Masahiro Tsuda, Mitsuru Hashida, Miku Konishi, Naoko Komura, Hiromune Ando, Fumiyoshi Yamashita.

Manuscript in preparation

References

1. Ehrhardt, C.; Kneuer, C.; Bakowsky, U. Selectins-an emerging target for drug delivery. Adv. Drug Delivery Rev. 2004, 56, 527-549.
2. Zhang, J.; Alcaide, P.; Liu, L.; Sun, J.; He, A.; Luscinskas, F. W.; Shi, G. P. Regulation of Endothelial Cell Adhesion Molecule Expression by Mast Cells, Macrophages, and Neutrophils. PLoS One 2011, 6, e14525.
3. Ray, K. P.; Farrow, S.; Daly, M.; Talabot, F.; Searle, N. Induction of the E-selectin promoter by interleukin 1 and tumour necrosis factor alpha, and inhibition by glucocorticoids. Biochem. J. 1997, 328, 707-715.
4. Narita, T.; Kimura, N. K.; Kasai, Y.; Hosono, J.; Nakashio, T.; Matsuura, N.; Sato, M.; Kannagi, R. Induction of E-selectin expression on vascular endothelium by digestive system cancer cells. J. Gastroenterol. 1996, 31, 299-301.
5. Eichbaum, C.; Meyer, A. S.; Bischofs, E.; Steinborn, A.; Bruckner, T.; Brodt, P.; Sohn, C.; Eichbaum, M. H. R. Breast cancer cell-derived cytokines, macrophages and cell adhesion: Implications for metastasis. Anticancer Res. 2011, 31, 3219-3228.
6. Khatib, A. M.; Kontogiannea, M.; Fallavollita, L.; Jamison, B.; Meterissian, S.; Brodt, P. Rapid induction of cytokine and E-selectin expression in the liver in response to metastatic tumor Cells. Cancer. Res. 1999, 59, 1356-1361.
7. Ma, S.; Tian, X. Y.; Zhang, Y.; Mu, C.; Shen, H.; Bismuth, J.; Pownall, H. J.; Huang, Y.; Wong, W. T. E-selectin-targeting delivery of microRNAs by microparticles ameliorates endothelial inflammation and atherosclerosis. Sci. Rep. 2016, 6, 22910.
8. Kang, H. W.; Josephson, L.; Petrovsky, A.; Weissleder, R.;Bogdanov, A. Magnetic resonance imaging of inducible E-selectin expression in human endothelial cell culture. Bioconjugate Chem. 2002, 13, 122-127.
9. Barthel, S. R.; Gavino, J. D.; Descheny, L.; Dimitroff, C. J. Targeting selectins and selectin ligands in inflammation and cancer. Expert Opin. Ther. Targets 2007, 11, 1473-1491.
10. Bhaskar, V.; Law, D. A.; Ibsen, E.; Breinberg, D.; Cass, K. M.; Dubridge, R. B.; Evangelista, F.; Henshall, S. M.; Hevezi, P.; Miller, J. C.; Pong, M.; Powers, R.; Senter, P.; Stockett, D.; Sutherland, R. L.; Jeffry, U. V.; Willhite, D.; Murray, R.; Afar, D. E. H.; Ramakrishnan, V. E Selectin up-regulation allows for targeted drug delivery in prostate cancer. Cancer. Res. 2003, 63, 6387-6394.

11. Kuznetsova, N. R.; Stepanova, E. V.; Peretolchina, N. M.; Khochenkov, D. A.; Boldyrev, I. A.; Bovin, N. V.; Vodovozova, E. L. Targeting liposomes loaded with melphalan prodrug to tumour vasculature via the Sialyl Lewis X selectin ligand. J. Drug Target. 2014, 22, 242-250.
12. Vodovozova, E. L.; Moiseeva, E. V.; Grechko, G. K.; Gayenko, G. P.; Nifant'ev, N. E.; Bovin, N. V.; Molotkovsky, J. G. Antitumour activity of cytotoxic liposomes equipped with selectin ligand SiaLex, in a mouse mammary adenocarcinoma model. Eur. J. Cancer 2000, 36, 942-949.
13. DeFrees, S. A.; Phillips, L.; Guo, L.; Zalipsky, S. Sialyl Lewis X liposomes as a multivalent ligand and inhibitor of E-selectin mediated cellular adhesion. J. Am. Chem. Soc. 1996, 118, 6101-6104.
14. Alekseeva, A.; Kapkaeva, M.; Shcheglovitova, O.; Boldyrev, I.; Pazynina, G.; Bovin, O.; Vodovozova, E. Interactions of antitumour sialyl Lewis X liposomes with vascular endothelial cells. Biochim. Biophys. Acta, Biomembr. 2015, 1848, 1099-1110.
15. Minaguchi, J.; Oohashi, T.; Inagawa, K.; Ohtsuka, A.; Ninomiya, Y. Transvascular accumulation of Sialyl Lewis X conjugated liposome in inflamed joints of collagen antibody-induced arthritic (CAIA) mice. Arch. Histol. Cytol. 2008, 71, 195-203.
16. Zalipsky, S.; Mullah, N.; Harding, J. A.; Gittelman, J.; Guo, L.; DeFrees, S. A. Poly(ethylene glycol)-grafted liposomes with oligopeptide or oligosaccharide ligands appended to the termini of the polimer chains. Bioconjugate Chem. 1997, 8, 111-118.
17. Danishefsky, S. J.; Gervay, J.; Peterson, J. M.; McDonald, F. E.; Koseki, K.; Griffith, D. A.; Oriyama, T.; Marsden, S. P. Application of glycols to the synthesis of oligosaccharides: convergent total syntheses of the Lewis X trisaccharide Sialyl Lewis X antigenic determinant and higher congeners. J. Am. Chem. Soc. 1995, 117, 1940-1953.
18. Ellervik, U.; Magnusson, G. A high yielding chemical synthesis of Sialyl Lewis X tetrasaccharide and Lewis X trisaccharide; examples of regio- and sterio differentiated glycosylations. J. Org. Chem. 1998, 63, 9314-9322.
19. Palcic, M. M.; Venot, A. P.; Ratcliffe, R. M.; Hindsgaul, O. Enzymic synthesis of oligosaccharides terminating in the tumor associated Sialyl-Lewis-a determitant. Carbohydr. Res. 1989, 190, 1-11.

20. Ball, G. E.; O'Neill, R. A.; Schultz, J. E.; Lowe, J. B.; Weston, B. W.; Nagy, J. O.; Brown, E.G.; Hobbs, C. J.; Bednarski, M. D. Synthesis and structural analysis using 2-D NMR of Sialyl Lewis X (SLex) and Lewis X (Lex) oligosaccharides: ligands related to E-selectin [ELAM-1] binding. J. Am. Chem. Soc. 1992, 114, 5449-5451.
21. Bendas, G.; Krause, A.; Schmidt, R.; Vogel, J.; Rothe, U. Selectins as new targets for immunoliposome-mediated drug delivery: A potential way of anti-inflammatory therapy. Pharm. Acta. Helv. 1998, 73, 19-26.
22. Kessner, S.; Krause, A.; Rothe, U.; Bendas, G. Investigation of the cellular uptake of E-selectin-targeted immunoliposomes by activated human endothelial cells. Biochim. Biophys. Acta. 2001, 1514, 177-190.
23. Spragg, D. D.; Alford, D. R.; Greferath, R.; Larsen, C. E.; Lee, K. D.; Gurtner, G. C.; Cybulsky, M. I.; Tosi, P. F.; Nicolau, C.; Gimbrone Jr. M. A. Immunotargeting of liposomes to activated vascular endothelial cells: a strategy for site-selective delivery in the cardiovascular system. Proc. Natl. Acad. Sci. U.S.A. 1997, 94, 8795-8800.
24. Dickerson, J. B.; Blackwell, J. E.; Ou, J. J.; Shinde Patil, V. R.; Goetz, D. J. Limited adhesionof biodegradable microspheres to E- and P-selectin under flow. Biotechnol. Bioeng. 2001, 73, 500-509.
25. Blackwell, J. E.; Dagia, N. M.; Dickerson, J. B.; Berg, E. L.; Goetz, D. J. Ligand coated nanosphere adhesion to E- and P-selectin under static and flow conditions. Ann. Biomed. Eng. 2001, 29, 523-533.
26. Hashida, N.; Ohguroa, N.; Yamazakib, N.; Arakawac, Y.; Oikid, E.; Mashimoa, H.; Kurokawae, N.; Tanoa, Y. High-efficacy site-directed drug delivery system using sialyl-Lewis X conjugated liposome. Exp. Eye. Res. 2008, 86, 138-149.
27. Jubeli, E.; Moine, L.; Nicolas, V.; Barratt, G. Preparation of E-selectin-targeting nanoparticles and preliminary in vitro evaluation. Int. J. Pharm. 2012, 426, 291-301.
28. Ding, Y.; Li, S.; Nie, G. Nanotechnological strategies for therapeutic targeting of tumor vasculature. Nanomedicine. 2013, 8, 1209-1222.
29. Kasterena, S. I.; Campbellb, S. J.; Serresc, S.; Anthonyb, D. C.; Sibsonc, N. R.; Davisa, B. G. Glyconanoparticles allow pre-symptomatic in vivo imaging of brain disease. PNAS. 2009, 106, 18-23.

30. Harding, J. A.; Engbers, C. M.; Newman, M. S.; Goldstein, N. I.; Zalipsky, S. Immunogenicity and pharmacokinetic attributes of poly(ethylene glycol)-grafted immunoliposomes. Biochim. Biophys. Acta. 1997, 1327, 181-192.
31. Mann, A. P.; Tanaka, T.; Somasunderam, A.; Liu, X.; Gorenstein, D. G.; Ferrari, M. E-selectin-targeted porous silicon particle for nanoparticle delivery to the bone marrow. Adv. Mater. 2011, 23, 278-82.
32. Zalipsky, S.; Mullah, N.; Harding, J. A.; Gittelman, J.; Guo, L.; DeFrees, S. A. Poly(ethylene glycol)-grafted liposomes with oligopeptide or oligosaccharide ligands appended to the termini of the polimer chains. Bioconjug. Chem. 1997, 8, 111-118.
33. Danishefsky, S. J.; Gervay, J.; Peterson, J. M.; McDonald, F. E.; Koseki, K.; Griffith, D. A.; Oriyama, T.; Marsden, S. P. Application of glycals to the synthesis of oligosaccharides: convergent total syntheses of the Lewis X trisaccharide Sialyl Lewis X antigenic determinant and higher congeners. J. Am. Chem. Soc. 1995, 117, 1940-1953.
34. Ellervik, U.; Magnusson, G. A high yielding chemical synthesis of Sialyl Lewis X tetrasaccharide and Lewis X trisaccharide; examples of regio- and sterio differentiated glycosylations. J. Org. Chem. 1998, 63, 9314-9322.
35. Palcic, M. M.; Venot, A. P.; Ratcliffe, R. M.; Hindsgaul, O. Enzymic systhesis of oligosaccharides terminating in the tumor-associated Sialyl-Lewis-a determitant. Carbohydr. Res. 1989, 190, 1-11.
36. Neelu, K.; Bert, E. T. Design and Synthesis of Sialyl Lewisx Mimics as E- and P-Selectin Inhibitors. Med. Res. Rev. 2002, 22, 566-601.
37. Titz, A.; Patton, J.; Smiesko, M.; Radic, Z.; Schwardt, O.; Magnani, J. L.; Ernst, B. Probing the carbohydrate recognition domain of E-selectin: The importance of the acid orientation in sLex mimetics. Bioorg. Med. Chem. 2010, 18, 19-27.
38. Graves, B. J.; Crowther, R. L.; Chandran, C.; Rumberger, J. M.; Li, S.; Huang, K. S.; Presky, D. H.; Familletti, P. C.; Wolitzky, B. A.; Burns, D. K. Insight into E-selectin/ligand interaction from the crystal structure and mutagenesis of the lec/EGF domains. Nature. 1994, 367, 532-538.
39. Somers, W. S.; Tang, J.; Shaw, G. D.; Camphausen, R. T. Insights into the Molecular Basis of Leukocyte Tethering and Rolling Revealed by Structures of P- and E-Selectin Bound to SLeX and PSGL-1. Cell. 2000, 103, 467-479.

40. Preston, R. C.; Jakob, R. P.; Binder, F. P. C.; Sager, C. P.; Ernst, B.; Maier, T. E-selectin ligand complexes adopt an extended high-affinity conformation. J. Mol. Cell. Biol. 2016, 8, 62-72.

41. Wong, C. H.; Varas, F. M.; Hung, S. C.; Marron, T. G.; Lin, C. C.; Gong, K. W.; Schmidt, G. W. Small molecules as structural and functional mimics of Sialyl Lewis X tetrasaccharide in Selectin inhibition: A remarkable enhancement of inhibition by additional negative charge and/or hydrophobic Group. J. Am. Chem. Soc. 1997, 119, 8152-8158.

42. Simanek, E. E.; McGarvey, G. J.; Jablonowski, J. A.; Wong, C. H. Selectin-carbohydrate interactions: from natural ligands to designed mimics. Chem. Rev. 1998, 98, 833-862.

43. Sakagami, M.; Hotie, K.; Higashi, K.; Yamada, H.; Hamana, H. Syntheses and evaluation of biantennary oligosaccharide ligands mimicking Sialyl Lewis X. Chem. Pharm. Bull. 1999, 47, 1237-1245.

44. Brandley, B. K.; Kiso, M.; Abbas, S.; Nikrad, P.; Srivasatava, O.; Foxall, C.; Oda, Y.; Hasegawa, A. Structure-function studies on selectin carbohydrate ligands. Modifications to fucose, sialic acid and sulphate as a sialic acid replacement. Glycobiology. 1993, 3, 633-641.

45. Ohmoto, H.; Nakamura, K.; Inoue, T.; Kondo, N.; Inoue, Y.; Yoshino, K.; Kondo, H.; Ishida, H.; Kiso, M.; Hasegawa, A. Studies on selectin blocker. 1. structure-activitiy relationships of Sialyl Lewis X analogs. J. Med. Chem. 1996, 39, 1339-1343.

46. Rao, B. N.; Anderson, M. B.; Musser, J. H.; Gilbert, J. H.; Schaefer, M. E.; Foxall, C.; Brandley, B. K. Sialyl Lewis X mimics derived from a pharmacophore search are Selectin inhibitors with anti-inflammatory activity. J. Biol. Chem. 1994, 269, 19663-19666.

47. Papahadjopoulos, D.; Allen, T. M.; Gabizon, A.; Mayhew, E.; Matthay, K.; Huang, S. K.; Lee, K. D.; Woodle, M. C.; Lasic, D. D.; Redemann, C.; Martin, F. J. Sterically stabilized liposomes: improvements in pharmacokinetics and antitumor therapeutic efficacy. Proc. Natl. Acad. Sci. 1991, 88, 11460-11464.

48. Yamaoka, T.; Tabata, Y.; Ikada, Y. Distribution and tissue uptake of poly(ethylene glycol) with different molecular weights after intravenous administration to mice. J. Pharm. Sci. 1994, 83, 601-606.

49. Allen, T. M.; Hansen, G.; Martin, F.; Redeman, C.; Yau-Young, A. Liposomes containing synthetic lipid derivatives of poly(ethyleneglycol) show prolonged circulation half-lives in vivo. Biochim. Biophys. Acta. 1991, 1066, 29-36.
50. Klibanov, A. L.; Maruyama, K.; Torchilin, V. P.; Huang, L. Amphipathic polyethylene glycols effectively prolong the circulation time of liposomes. FEBS. Lett. 1990, 268, 235-237.
51. Jubeli, E.; Moine, L.; Gauduchon, J. V.; Barratt, G. E-selectin as a target for drug delivery and molecular imaging. J. Control. Release. 2012, 158, 194-206.
52. Wang, Y.; Yan, Q.; Wu, J.; Zhang, L. H.; Ye, X. S. A new one-pot synthesis of α-Gal epitope derivatives involved in the hyperacute rejection response in xenotransplantation. Tetrahedron. 2005, 61, 4313-43121.
53. Ishiwata, A.; Munemura, Y.; Ito, Y. Synergistic solvent effect in 1,2-cis-glycoside formation. Tetrahedron. 2008, 64, 92-102.
54. GROMACS version 5.0.4. http://www.gromacs.org/
55. Hornak, V.; Abel, R.; Okur, A.; Strockbine, B.; Roitberg, A.; Simmerling C. Comparison of multiple amber force fields and development of improved protein backbone parameters. Proteins. 2006, 65, 712-725.
56. Wang, J.; Wolf, R. M.; Caldwell, J. W. ; Kollman, P. A. ; Case III, D. A. Development and testing of a general amber force field. J. Comput. Phys. 2004, 25, 1157-1174.
57. Jakalian, A.; Bush, B. L.; Jack D. B.; Bayly C.I. Fast, efficient generation of high-quality atomic charges. AM1-BCC model: I. Method. J. Comp. Chem. 2000, 21, 132-146.
58. Jorgensen, W. L. Quantum and statistical mechanical studies of liquids. 10. Transferable intermolecular potential functions for water, alcohols, and ethers. Application to liquid water. J. Am. Chem. Soc. 1981, 103, 335-340.
59. Lu, D.; Hu, Y.; He, X.; Sollogoub, M.; Zhang, Y. Total synthesis of a sialyl Lewisx derivative for the diagnosis of cancer. Carbohydr. Res. 2014, 383, 89-96.
60. Chapman, P. T.; Yarwood, H.; Harrison, A. A.; Stocker, C. J.; Jamar, F.; Gundel, R. H.; Peters, A. M.; Haskard, D. O. Endothelial activation in monosodium urate monohydrate crystal-induced inflammation. In vitro and in vivo studies on the roles of tumor necrosis factor α and interleukin-1. Arthritis. Rheum. 1997, 40, 955-965.
61. Matharu, N. M.; Butler, L. M.; Rainger, G. E.; Gosling, P.; Vohra, R. K.; Nash, G. B. Mechanisms of the anti-inflammatory effects of hydroxyethyl starch

demonstrated in a flow-based model of neutrophil recruitment by endothelial cells. Crit. Care. Med. 2008, 36, 1536-1542.

62. Boyle, E. M. Jr.; Kovacich, J. C.; Canty, T. G. Jr.; Morgan, E. N.; Chi, E.; Verrier, E. D.; Pohlman, T. H. Inhibition of nuclear factor-kappa B nuclear localization reduces human E-selectin expression and the systemic inflammatory response. Circulation. 1998, 98, 282-288.
63. Onat, D.; Brillon, D.; Colombo, P. C.; Schmidt, A. M. Human vascular endothelial cells: A model system for studying vascular inflammation in diabetes and atherosclerosis. Curr. Diab. Rep. 2011, 11, 193-202.
64. Kim, I.; Moon, S. O.; Park, S. K.; Chae, S. W.; Koh, G. Y. Angiopoietin-1 reduces VEGF-stimulated leukocyte adhesion to endothelial cells by reducing ICAM-1, VCAM-1, and E-selectin expression. Circ. Res. 2001, 14, 477-479.
65. Wada, Y.; Saito, T.; Matsuda, N.; Ohmoto, H.; Yoshino, K.; Ohashi, M.; Kondo, H. Studies on selectin blockers. 2. Novel selectin blocker as potential therapeutics for inflammatory disorders. J. Med. Chem. 1996, 39, 2055-2059.
66. Rodgers, S. D.; Camphausen, R. T.; Hammer, D. A. Sialyl Lewis(x)-mediated, PSGL-1-independent rolling adhesion on P-selectin. Biophys. J. 2000, 79, 694-706.
67. Malý, P.; Thall, A. D.; Petryniak, B.; Rogers, C. E.; Smith, P. L.; Marks, R. M.; Kelly, R. J.; Gersten, K. M.; Cheng, G.; Saunders, T, L.; Camper, S. A.; Camphausen, R. T.; Sullivan, F. X.; Isogai, Y.; Hindsgaul, O.; Andrian, U. H.; Lowe, J. B. The α(1,3) Fucosyltransferase Fuc-TVII Controls Leukocyte Trafficking through an Essential Role in L-, E-, and P-selectin Ligand Biosynthesis. Cell. 1996, 86, 643-653.
68. Shodai, T.; Suzuki, J.; Kudo, S.; Itoh, S.; Terada, M.; Fujita, S. Shimazu, H.; Tsuji, T. Inhibition of P-selectin-mediated cell adhesion by a sulfated derivative of sialic acid. Biochem. Biophys. Res. Commun. 2003, 312, 787-793.
69. Yao, L.; Pan, J.; Setiadi, H.; Pate1, K. D.; McEver, R. P. Interleukin 4 or Oncostatin M induces a prolonged increase in P-Selectin mRNA and protein in Human endothelial cells. J. Exp. Med. 1996, 184, 81-92.
70. Foreman, K. E.; Vaporciyan, A. A.; Bonish, B. K.; Jones, M. L.; Johnson, K. J.; Glovsky, M. M.; Eddy, S. M.; Ward, P. A. C5a-induced expression of P-selectin in endothelial cells. J. Clin. Invest. 1994, 94, 1147-1155.
71. Thoma, G.; Magnani, J. L.; Patton, J. T. Synthesis and biological evaluation of a Sialyl Lewis X mimic with significantly improved E-selectin inhibition. Bioorg. Med. Chem. Lett. 2001, 11, 923-925.

72. Hanessian, S.; Reddy, G. V.; Huynh, H. K.; Pan, J.; Pedatella, S. Design and synthesis of sialyl Lex mimetics based on carbocyclic scaffolds derived from (–) quinic acid. Bioorg. Med. Chem. Lett. 1997, 7, 2729-2734.
73. Li, F.; Wilkins, P. P.; Crawley, S; Weinstein, J.; Cummings, R. D.; McEve, R. P. Post-translational modifications of recombinant P-selectin glycoprotein ligand-1 required for binding to P- and E-selectin. J. Biol. Chem. 1996, 271, 3255-3264.
74. Siemann, D. W.; Horsman, M. R. Vascular targeted therapies in oncology. Cell. Tissue. Res. 2009, 335, 1, 241-248.
75. Hanahan, D.; Weinberg, R. A. Hallmarks of cancer: the next generation. Cell. 2011, 144, 5, 646-74.
76. Chen, F.; Cai, W. Tumor Vasculature Targeting: A Generally Applicable Approach for Functionalized Nanomaterials. Small. 2014, 10, 1887-1893.
77. Staton, C. A.; Reed, M. W.; Brown, N. J. A critical analysis of current in vitro and in vivo angiogenesis assays. Int. J. Exp. Path. 2009, 90, 195-221.
78. Kurohane, K.; Tominaga, A.; Sato, K.; North, J. R.; Namba, Y.; Oku, N. Photodynamic therapy targeted to tumor-induced angiogenic vessels. Cancer Lett. 2001, 167, 49-56.
79. Takeuchi, Y.; Kurohane, K.; Ichikawa, K.; Yonezawa, S.; Nango, M.; Oku, N. Induction of Intensive Tumor Suppression by Antiangiogenic Photodynamic Therapy Using Polycation-Modified Liposomal Photosensitizer. Cancer. 2003, 97, 8, 2027-2034.
80. Ohkouchi, K.; Imoto, H.; Takakura, Y.; Hashida, M.; Sezaki, H. Disposition of Anticancer Drugs after Bolus Arterial Administration in a Tissue-isolated Tumor Perfusion System. Cancer Res. 1990, 50, 1640-1644.
81. Biel, N. M.; Lee, J. A.; Sorg, B. S.; Siemann, D. W. Limitations of the dorsal skinfold window chamber model in evaluating anti-angiogenic therapy during early phase of angiogenesis. Vascular Cell. 2014, 6, 17, 1-11.
82. Staton, C. A.; Reed, M. W.; Brown, N. J. A critical analysis of current in vitro and in vivo angiogenesis assays. Int. J. Exp. Path. 2009, 90, 195-221.
83. Li, T.; Kang, G.; Wang, T.; Huang, H. Tumor angiogenesis and anti-angiogenic gene therapy for cancer. Oncol. Lett. 2018, 16, 687-702.
84. Dutour, A.; Rigaud, M. Tumor endothelial cells are targets for selective therapies: in vitro and in vivo models to evaluate antiangiogenic strategies. Anticancer Res. 2005, 25, 3799-3808.

85. Samant, R. S.; Shevde, L. A. Recent advances in anti-angiogenic therapy of cancer. Onco. Target. 2011, 2, 122-134.
86. Bergers, G.; Hanahan, D. Modes of resistance to anti-angiogenic therapy. Nat. Rev. Cancer. 2008, 8, 592-603.
87. Ma, S.; Pradeep, S.; Hu, W.; Zhang, D.; Coleman, R.; Sood, A. The role of tumor microenvironment in resistance to anti-angiogenic therapy. F1000 Res. 2018, 326, 7, 1-19.
88. Abdalla, A. M. E.; Xiao, L.; Ullah, M. W.; Yu, M.; Ouyang, C.; Yang, G. Current challenges of cancer anti-angiogenic therapy and the promise of nanotherapeutics. Theranos. 2018, 8, 2, 533–548.
89. Tan, F.; Mo, X. H.; Zhao, J.; Liang, H.; Chen, Z. J.; Wang, X. L. A novel delivery vector for targeted delivery of the antiangiogenic drug paclitaxel to angiogenic blood vessels: TLTYTWS-conjugated PEG–PLA nanoparticles. J. Nanopart. Res. 2017, 19, 51.
90. Murphy, E. A.; Majeti, B. K.; Barnes, L. A.; Makale, M.; Weis, S. M., Lutu-Fuga, K.; Wrasidlo, W.; Cheresh, D.A. Nanoparticle-mediated drug delivery to tumor vasculature suppresses metastasis. Proc. Natl. Acad. Sci. USA. 2008, 105, 9343-9348.
91. Zhu, S.; Kisiel, W.; Lu, Y. J.; Petersen, L. C.; Ndungu, J. M.; Moore, T. W.; Parker, E. T.; Sun, A.; Liotta, D. C.; El-Rayes, B. F.; Brat, D. J.; Snyder, J. P.; Shoji, M. Tumor angiogenesis therapy using targeted delivery of paclitaxel to the vasculature of breast cancer metastases. J. Drug Deliv. 2014, 865732.